CHAPTER 2

MATERIALS & METHODS

This chapter provides details of experiments for structural study in solid state by X-ray crystallography and for dynamical study in liquid state by neutron scattering.

2.1 Materials

DIMEB and TRIMEG were purchased from Cyclolab (Budapest, Hungary) except for the X-ray diffraction experiment with DIMEB·$2H_2O$, from Aldrich (Steinheim, Germany). They were used without further purification or were re-crystallized, if necessary, from hot water. Besides methylated CDs, γ-CD obtained from Carl Roth (Karlsruhe, Germany) were used for the neutron scattering experiment.

2.2 X-Ray Crystallographic Method

X-ray crystallography is a standard tool to elucidate the three dimensional structure of a substance which can be obtained as single crystal. For small molecule with molecular weight less than 5000, the first step of an X-ray analysis is crystallization by evaporation of solvent or related methods. The second step is determining the unit cell constants and the space group of a suitable single crystal (ideally, 0.2–0.5 mm in each dimension) by measuring the spacing and checking the systematic absences of reflections in the recorded diffraction pattern. Next step is collecting the X-ray diffraction data, afterward the raw data is reduced and corrected for effects of absorption and polarization to obtain the unique data set. The crucial step is to solve the "phase problem" and to determine the structure (getting a "trial structure" or approximate phase angles) in which many programs can be employed to

accomplish this step depending on direct methods or molecular replacement to be used. The last step is structure refinement, the "trial" structure which is chemically reasonable (contains 60–80% of the total number of non-hydrogen atoms in the complete structure) from the previous step is extended to find all remaining non-hydrogen atoms. The final refined structure should have a low residual index, R (ideally, $\approx$ 3–5%) which is an indication for the precision of collected data and correctness of the structure (good agreement between observed and calculated structure factors). The details of X-ray structure determination can be found in many crystallographic textbooks [61, 105, 164].

For the crystal structures of DIMEB and TRIMEG described in this thesis, their geometrical parameters were calculated by PARST-96 [125]. The structure illustrations were produced by MOLSCRIPT [103] for the ball-and-stick presentation in chapter 3, by ORTEP-III [24] for the thermal ellipsoids plots in Appendix A, and by SCHAKAL-88 [96] for Figure 3.6 on page 60.

2.2.1 Crystallographic Experiment of DIMEB

2.2.1.1 DIMEB·2H_2O

Crystallization. A saturated aqueous solution of DIMEB was prepared at –5°C and transferred to 18°C. After 2 months, rod shaped colorless crystals, up to 1.5 mm in length, had grown by slow solvent evaporation.

X-ray Diffraction Experiment. A crystal, 0.2×0.5×1.5 mm^3 in dimensions, was mounted in a quartz capillary. A total of 16750 X-ray diffraction data were collected at room temperature using a Bruker-AXS CCD area detector equipped with graphite-monochromatized MoK_α radiation ($\lambda = 0.71073$ Å). Data reduction was carried out with the program SAINT [151], including semiempirical absorption correction ($\mu = 0.1\ mm^{-1}$) with SADABS [147]; symmetry equivalent reflections were merged to yield 5606 unique data. The crystals belong to the monoclinic space group $P2_1$ with unit cell dimensions: $a = 15.2415(5)$, $b = 10.6391(4)$, $c = 23.3239(8)$ Å, $\beta = 101.798(1)°$; the formula per asymmetric unit is $C_{56}H_{98}O_{35}\cdot 2H_2O$.

Structure Solution and Refinement. The crystal structure was determined by direct methods [5], developed by Fourier synthesis [148] and refined by full-matrix

least squares techniques [148]. All non-hydrogen atoms were refined anisotropically. The C–H and O3–H hydrogen atoms of the glucoses were calculated into idealized positions and, during refinement, restrained according to the "riding model" [148]. The high thermal displacement factors of the methoxy groups made refinement difficult. Twofold disorder was observed for O6–C8 of glucose residue 3 (see Figure 3.1 on page 52). Water W1 is included in the cavity and has a very high thermal displacement factor (U_{eq} = 0.72 Å^2) due to lack of interactions with DIMEB, while W2 is located in interstices between DIMEB molecules and hydrogen-bonded to O3 and O6 atoms (U_{eq} = 0.18 Å^2), see ORTEP plot on page 108 and list of isotropic temperature factors on page 110. The refinement of 944 parameters converged at a final $R(F^2)$ = 0.078 for all 5606 data. Details of the crystallographic data are given in Table 2.1. The final fractional atomic coordinates and equivalent isotropic thermal displacement factors are listed in Table A.1 on page 110.

2.2.1.2 DIMEB·15H$_2$O

Crystallization. A concentrated aqueous solution of DIMEB prepared in water at 0°C was stored at 18°C. After two months, prismatic crystals were obtained by slow water evaporation.

X-ray Diffraction Experiment. A crystal of 0.4×0.5×2.0 mm^3 was sealed in a quartz capillary, and 37113 X-ray reflections were collected at room temperature to 0.9 Å resolution on a Bruker-AXS CCD area detector using graphite-monochromatized MoK$_\alpha$ radiation (λ = 0.71073 Å), including semiempirical absorption correction from ψ-scans (μ = 0.11 mm^{-1}) and data reduction (with programs SAINT [151]) and SHELXTL [152] yielded 6760 unique reflections. The crystal spece group is orthorhombic $P2_12_12_1$ with unit cell dimensions: a = 14.1632(5), b = 20.8278(7), c = 29.2611(10) Å. There are one DIMEB and 15 water molecules in the asymmetric unit, see Table 2.1.

Structure Solution and Refinement. The structure was determined by direct methods (SHELXS-97 [149]) and refined by full-matrix least-squares on F^2 (SHELXL-97 [148]). All non-hydrogen atoms were treated anisotropically. Most of the hydrogen atoms of the β-CD skeleton and some of the water molecules could be located and

were refined isotropically – positions of the methyl and hydroxyl hydrogen atoms were calculated according to the "riding model" [148]; at glucose unit 2, a methyl group was located with 0.25 occupation (due to impurity as verified by mass spectrometry, not shown). All 15 water sites were found fully occupied. The refinement of 1110 parameters converged at a final $R = 0.069$, $wR = 0.177$ for 5725 data with $F^2 > 2\sigma(F^2)$, the highest peak and deepest hole are 0.32 and –0.23 e $Å^{-3}$ in the final difference electron density. Summary of the crystallographic data is given in Table 2.1. The final fractional atomic coordinates and equivalent isotropic thermal displacement factors are listed in Table A.2 on page 111.

Thermal Analysis. A DIMEB·15H_2O crystal was mounted in an Enraf-Nonius heating device installed on a Mar Research imaging plate. The same diffraction pattern with 5° oscillation range was taken at 10°C intervals from 20–310°C using CuK_α radiation from Enraf Nonius FR571 X-ray generator with rotating anode. Unit cell constants evaluated with DENZO [128] showed phase transition at 110°C (changes of unit cell parameters), and decomposition (loss of X-ray diffraction) above 280°C. For differential scanning calorimetry, 10 mg of powdered DIMEB·15H_2O were enclosed in an aluminium pan and heated in a Netsch Instruments apparatus from –100 to 350°C. Phase transition occurred at 111°C and decomposition above 280°C.

Table 2.1: Crystallographic data of DIMEB

DIMEB obtained from cold water at 18°C in two crystal forms: DIMEB·$2H_2O$ in monoclinic $P2_1$ and DIMEB·$15H_2O$ in orthorhombic $P2_12_12_1$.

Compound	DIMEB·$2H_2O$	DIMEB·$15H_2O$
Chemical formula	$C_{56}H_{98}O_{35}\cdot 2H_2O$	$C_{56.25}H_{97.75}O_{35}\cdot 15H_2O$
Formula weight	1363.36	1604.35
Crystal habit, color	rod, colorless	rod, colorless
Crystal size (mm^3)	0.2×0.5×1.5	0.4×0.5×2.0
Crystal system	monoclinic	orthorhombic
Space group	$P2_1$	$P2_12_12_1$
Unit cell dimensions		
a (Å)	15.2415(5)	14.1632(5)
b (Å)	10.6391(4)	20.8278(7)
c (Å)	23.3239(8)	29.2611(10)
β (°)	101.798(1)	90
Volume ($Å^3$)	3702.2(2)	8631.7(5)
Z	2	4
D_x (g cm^{-3})	1.22	1.21
μ (mm^{-1})	0.10	0.11
$F(000)$	1460	3357
Diffractometer	Bruker, CCD	Bruker, CCD
Wavelength (MoK_α, Å)	0.71073	0.71073
Temperature (°C)	20	20
Θ for data collection (°)	0.89–23.31	1.20–23.38
Resolution (Å)	0.90	0.90
Measured reflections	16748	37113
Unique reflections (all data)	5603 ($R_{int} = 0.0608$)	6760 ($R_{int} = 0.0838$)
Unique reflections $[F^2 > 2\sigma(F^2)]$	5036	5725
Index ranges	$-16 \le h \le 16$ $0 \le k \le 11$ $0 \le l \le 25$	$0 \le h \le 15$ $0 \le k \le 23$ $0 \le l \le 32$
Structure solution	direct methods (SIR-92)	direct methods (SHELXS-97)
Refinement method	full-matrix least-squares on F^2	full-matrix least-squares on F^2
Weighting scheme	$w = [S^2(F_o^2) + (0.1402P)^2 + 1.2456P]^{-1}$ where $P = (F_o^2 + 2F_c^2)/3$	$w = [S^2(F_o^2) + (0.1103P)^2 + 3.1150P]^{-1}$ where $P = (F_o^2 + 2F_c^2)/3$
Data/parameters	5603/944	6760/1100
R $[F^2 > 2\sigma(F^2)]$	$R^a = 0.074$, $wR^b = 0.190$	$R = 0.069$, $wR = 0.177$
R (all data)	$R = 0.081$, $wR = 0.202$	$R = 0.081$, $wR = 0.191$
Goodness of fit	1.085	1.128
Highest peak/ deepest hole (e $Å^{-3}$)	0.65/–0.38	0.32/–0.23

[a] $R = \Sigma||F_o| - |F_c||/\Sigma|F_o|$. [b] $wR = \{w(F_o^2 - F_c^2)^2/w(F_o^2)^2\}^{1/2}$.

2.2.2 Crystallographic Experiment of TRIMEG

2.2.2.1 (4TRIMEG)·19.3H_2O

Crystallization. A saturated aqueous solution of TRIMEG was prepared at 0°C and kept at 4°C for about one month, but no crystals formed. However, when the vials containing these solutions were transferred to a microscope at 18°C for visual inspection, large prisms 3×3×4 mm^3 in size crystallized spontaneously within 30 minutes.

X-ray Diffraction Experiment. A crystal of 0.3×0.7×1.0 mm^3 was sealed together with a drop of mother liquor in a quartz capillary and used for X-ray data collection performed at room temperature with a Bruker-AXS SMART diffractometer equipped with a CCD area detector using graphite-monochromated MoK_α-radiation, $\lambda = 0.71073$ Å. The 77093 data were collected in the Θ range 1.42–23.78° (0.88 Å resolution). Data reduction and semiempirical absorption correction from ψ-scans were carried out using the programs SAINT [151] and SHELXTL [152], to yield 19782 reflections with $F^2 > 2\sigma(F^2)$. Space group is monoclinic $P2_1$ according to systematic absences of all $0k0$ reflections with k odd, crystal unit cell dimensions are a = 29.8717(9), b = 18.0183(6), c = 33.1696(11) Å, β = 98.147(1)° and there are four TRIMEG molecules and a total of 19.3 water molecules in the asymmetric unit (see Table 2.2).

Structure Solution and Refinement. Several attempts to determine the structure failed. In molecular replacement, the TRIMEG·2H_2O [160] phasing model was too different from TRIMEG in this crystal structure as found later, and in direct methods the success rate falls off above 150 atoms (four TRIMEG have 448 C and O atoms). The structure was finally determined by a novel "*ab initio*" real/reciprocal space recycling procedure [146] implemented in SHELXD. It is inspired by, but different in detail from the "shake and bake" method [122]. It provided all TRIMEG C and O atoms except for some disordered methyl groups and several of the water O atoms. The remaining atoms were located from difference Fourier maps. Due to the large structure (467 non-hydrogen atoms) and the relatively low data/parameter ratio, refinement strategies were similar to those for macromolecular crystal structures utilizing distance and displacement parameter restraints and block-matrix conjugate

gradient least squares on F^2 as implemented in SHELXL-97 [148]. The option SADI was employed to improve the geometry of each of the 32 glucose units by restraining the corresponding 1,2- and 1,3-distances to be equal. Water sites and disordered methyl groups were located from difference electron density maps, C–H hydrogen atoms were placed in calculated positions – those of water could not be determined. All non-hydrogen atoms were treated anisotropically, refinement of 4341 parameters against 19782 data with $F^2 > 2\sigma(F^2)$ converged at $R = 0.084$, see Table 2.2.

As shown in Figures 3.8(a)–(d) (page 66), 3.9(a) (page 67), Tables 3.3(b) and (c) (page 62), several of the methyl and O6–CH_3 groups are twofold disordered. These are O63–C93 and O64–C94 in TRIMEG 2; C76, C96, and O68 in TRIMEG 4. The 19.3 water molecules are distributed over 27 sites with occupation factors in the range 0.18–1.00, see Figures 3.10(a)–(c) on page 69.

2.2.2.2 TRIMEG·4.5H_2O

Crystallization. A concentrated solution of TRIMEG in cold water was kept at 0°C for a month, but no crystals formed. To enforce crystallization, the solution was heated to 80°C. In contrast to other experiments which afforded crystallization of TRIMEG·2H_2O [160] under these conditions, the solution became highly viscous. When the solution was cooled to 18°C after 30 minutes, it remained viscous and rod-shaped crystals were obtained after one week.

X-ray Diffraction Experiment. A crystal was mounted in a quartz capillary for X-ray diffraction experiments performed at room temperature with a Bruker-AXS CCD area detector using graphite-monochromatized MoK_α-radiation, see Table 2.2. Semiempirical absorption correction using ψ-scans and data reduction were accomplished with programs SAINT [151] and SHELXTL [152], and merged to yield 5779 unique reflections.

Structure Solution and Refinement. The crystal structure was determined by direct methods with program SHELXS-97 [149], developed by difference Fourier techniques, and refined by full-matrix least-squares on F^2 [148]. All hydrogen atoms of TRIMEG were put in the standard geometry according to the "riding model" [148] – those of the water molecules could not be determined. The TRIMEG methoxy groups

and disordered water molecules show excessive thermal parameters. After the 1096 atomic parameters (atomic coordinates and anisotropic temperature factors) were refined against 4311 data with $F^2 > 2\sigma(F^2)$, the *R*-factor converged at 0.104. The total of 4.5 water molecules located within the central cavity of TRIMEG are distributed over 15 positions (occupancy factors 0.25–0.60, see caption Figure 3.11 on page 71). The relatively high *R*-factor may be due to instability of the crystals which tended to dry out during data collection, resulting in a large number of weak X-ray data at high resolution. A summary of crystallographic data is given in Table 2.2.

Table 2.2: Crystallographic data of TRIMEG

TRIMEG obtained from cold water at 18°C in two crystal forms: (4TRIMEG)·19.3H_2O in monoclinic $P2_1$ and TRIMEG·4.5H_2O in orthorhombic $P2_12_12_1$.

Compound	(4TRIMEG)·19.3H_2O	TRIMEG·4.5H_2O
Chemical formula	(4$C_{72}H_{128}O_{40}$)·19.3H_2O	$C_{72}H_{128}O_{40}$·4.5H_2O
Formula weight	6843.66	1705.74
Crystal habit, color	plate, colorless	rod, colorless
Crystal size (mm^3)	0.3×0.7×1.0	0.2×0.2×0.5
Crystal system	monoclinic	orthorhombic
Space group	$P2_1$	$P2_12_12_1$
Unit cell dimensions		
a (Å)	29.8717(9)	10.7879(3)
b (Å)	18.0183(6)	29.0580(9)
c (Å)	33.1696(11)	32.2909(11)
β (°)	98.147(1)	90
Volume ($Å^3$)	17673(4)	10122.4(5)
Z	2	4
D_x (g cm^{-3})	1.29	1.12
μ (mm^{-1})	0.11	0.09
F(000)	7349	3664
Diffractometer	Bruker, CCD	Bruker, CCD
Wavelength (MoK_α, Å)	0.71073	0.71073
Temperature (°C)	20	25
Θ for data collection (°)	1.42–23.78	2.01–20.82
Resolution (Å)	0.88	1.00
Measured reflections	77093	31669
Unique reflections (all data)	26821 (R_{int} = 0.0317)	5779 (R_{int} = 0.1065)
Unique reflections $[F^2 > 2\sigma(F^2)]$	19782	4311
Index ranges	$-33 \le h \le 32$ $0 \le k \le 20$ $0 \le l \le 37$	$0 \le h \le 10$ $0 \le k \le 29$ $0 \le l \le 32$
Structure solution	*ab initio* methods (SHELXD)	direct methods (SHELXS-97)
Refinement method	distance and displacement parameter restraints and block matrix conjugate-gradient least-square on F^2	full-matrix least-squares on F^2
Weighting scheme	$w = [S^2(F_o^2) + (0.0915P)^2 + 17.5934P]^{-1}$ where $P = (F_o^2 + 2F_c^2)/3$	$w = [S^2(F_o^2) + (0.0962P)^2 + 15.0416P]^{-1}$ where $P = (F_o^2 + 2F_c^2)/3$
Data/parameters	26821/4341	5779/1080
R $[F^2 > 2\sigma(F^2)]$	R^a = 0.084, wR^b = 0.203	R = 0.104, wR = 0.220
R (all data)	R = 0.110, wR = 0.222	R = 0.134, wR = 0.239
Goodness of fit	1.062	1.146
Highest peak/ deepest hole (e $Å^{-3}$)	0.65/–0.39	0.26/–0.25

[a] $R = \Sigma||F_o| - |F_c||/\Sigma|F_o|$. [b] $wR = \{w(F_o^2 - F_c^2)^2/w(F_o^2)^2\}^{1/2}$.

2.3 Neutron Scattering Method

2.3.1 Sample Preparation

DIMEB, TRIMEG and γ-CD were separately dissolved in distilled water (H_2O) that had been passed through a 0.22 μm filter (Millipore Corp.), to reach a concentration of 37.6 mM which corresponds to 500 mg DIMEB, 614 mg TRIMEG, and 487 mg γ-CD in 10 mL water each. These solutions were freshly prepared and filled in the rectangular slab-shaped aluminium cans with 5 cm width, 10 cm height, and 0.02 cm thickness.

2.3.2 Neutron Scattering Experiment

The spectra of all samples (CD solutions and pure water) were recorded at three different temperatures $T = 287$, 305, and 323 K using the time-of-flight (TOF) spectrometer NEAT (Hahn-Meitner-Institut, Berlin) with an incident wavelength of $\lambda_0 = 5.1$ Å (produced by controlling the speed of 7 phased disk choppers), elastic energy resolution $\Delta E = 100$ μeV (full width at half maximum, FWHM), with an array of 388 single detectors extending in a scattering angle range of $13.3° \leq \phi \leq 136.7°$; this corresponds to a wave vector range of 0.28–2.27 Å^{-1} for an elastic momentum transfer ($Q = 4\pi sin(\phi/2)/\lambda_0$). The calculated sample transmissions in the direction perpendicular to the slab plane are about 0.9. The measurement time for each sample of 3–5 hours is sufficient to obtain good statistics of the data. To ensure that the measured signal is dominated by incoherent neutron scattering of H-atoms, the sample orientation angle $\alpha = 45°$ with respect to the direction of the incident neutron beam was used for all measurements (samples, vanadium standard, and empty can). All TOF spectra were corrected, normalized, sampled in 20 groups, transformed to the energy transfer scale, and analysed using the program package FITMO-2 [45].

2.3.3 Theory of Data Analysis

In a neutron scattering experiment, the measured quantity is the double differential cross section, $d^2\sigma$ which is the probability that a neutron with incident energy E_0 leaves the sample in the solid angle $d\vec{\Omega}$ in the direction $\vec{\Omega}$ and with an energy exchange

between $\hbar\omega$ and $\hbar(\omega + d\omega)$:

$$\frac{d^2\sigma}{d\vec{\Omega}d\omega} = \frac{\vec{k}}{4\pi N\vec{k}_0} S(\vec{Q},\omega) \tag{2.1}$$

where $\vec{k}_0$ and $\vec{k}$ are neutron wave vectors before and after the scattering process, N is the number of scattering neutron atoms, $\vec{Q}$ is the momentum transfer vector (= $\vec{k}$ – $\vec{k}_0$), and $S(\vec{Q},\omega)$ is the neutron scattering function. The scattering process is due to the interference between waves originating from the same and different nuclei called *incoherent* and *coherent* scattering, respectively. Therefore, the total scattering function comprises two terms:

$$S(\vec{Q},\omega) = \sigma_{inc} S_{inc}(\vec{Q},\omega) + \sigma_{coh} S_{coh}(\vec{Q},\omega) \tag{2.2}$$

Because of the very large incoherent scattering cross-section of H-atoms, i.e., σ_{inc}(H) = 79.9 [barns] compared to σ_{inc}(D) = 2.04, σ_{inc}(C) = 0.001, σ_{inc}(O) = 0.000, σ_{inc}(N) = 0.49; the total scattering function is approximated to the incoherent scattering function which gives information on dynamic properties of the hydrogenous molecules. The measured scattering intensity is proportional to the incoherent scattering function $S_{inc}(\vec{Q},\omega)$ which is the space and time Fourier transform of the self correlation function $G_s(\vec{r}$,t), developed by Van Hove [85]:

$$S_{inc}(\vec{Q},\omega) = \frac{1}{2\pi}\int_{-\infty}^{\infty} e^{-i\omega t}\int_{-\infty}^{\infty} e^{i\vec{Q}\vec{r}} G_s(\vec{r},t)d\vec{r}dt \tag{2.3}$$

In the classical approximation (further details see [14, 106]), $G_s(\vec{r},t)$ describes the average time-dependent probability density distribution of H-atoms,

$$G_s(\vec{r},t) = \frac{1}{N}\sum_{i=1}^{N}\langle\delta[\vec{r} + \vec{R}_i(0) - \vec{R}_i(t)]\rangle \tag{2.4}$$

where $\vec{R}_i(0)$ and $\vec{R}_i(t)$ are position vectors of atom i for the time $t = 0$ and for time t. Because the atomic trajectories cannot be directly calculated from the measured scattering function, the analytical models are used in practice to investigate the movements of individual atoms (see for example [14]). This is a traditional treatment of neutron scattering data in which a calculated theoretical scattering function, $S_{theo}(\vec{Q},\omega)$ is fitted to a measured scattering function, $S_{meas}(\vec{Q},\omega)$ as follow:

$$S_{meas}(\vec{Q},\omega) = F_N e^{-\frac{\hbar\omega}{2k_BT}}[S_{theo}(\vec{Q},\omega)\otimes S_{res}(\vec{Q},\omega)] \tag{2.5}$$

where F_N is the normalization factor, $e^{-\frac{\hbar\omega}{2k_BT}}$ is the detailed balance factor, $S_{res}(\vec{Q},\omega)$ is the resolution function obtained from vanadium measurement as standard for pure elastic incoherent scattering, and $\otimes$ is the energy convolution operator.

2.3.4 Data Analysis of CD Solution

In the present study, the calculated transmission perpendicular to the slab plane is quite high (0.9), indicating that in principle, the effect of multiple neutron scattering is negligible. Since in the data analysis of pure water, the best fit with reasonable parameters could not be obtained, the multiple scattering correction has been introduced to the analytical model of pure water which is a bulk water component in the CD solution.

$S_{theo}(\vec{Q},\omega)$ of a CD solution can be decomposed into three fractions. They are the scattering functions from the H-atoms of bulk water, $S_{bulk}(\vec{Q},\omega)$; of hydration water, $S_{hyd}(\vec{Q},\omega)$; of CD molecules, $S_{CD}(\vec{Q},\omega)$. The contribution from inelastic scattering is taken into account by the damped harmonic oscillator (DHO) scattering function, $S_{DHO}(\omega)$ [174]. Hence,

$$\begin{aligned} S_{theo}(\vec{Q},\omega) &= e^{-\langle u^2\rangle Q^2}\{F_{bulk}[F_{SSC}S_{bulk}(\vec{Q},\omega) + F_{MSC}S_{MSC}(\vec{Q},\omega)] + \\ & \quad F_{SSC}[F_{hyd}S_{hyd}(\vec{Q},\omega) + F_{CD}S_{CD}(\vec{Q},\omega) + S_{DHO}(\omega)]\} \end{aligned} \tag{2.6}$$

where

$$F_{hyd}S_{hyd}(\vec{Q},\omega) = F^{in}_{hyd}S^{in}_{hyd}(\vec{Q},\omega) + F^{out}_{hyd}S^{out}_{hyd}(\vec{Q},\omega) \tag{2.7}$$

$F_{SSC} = 1/(2 - T_\alpha)$ and $F_{MSC} = (1 - T_\alpha)/(2 - T_\alpha)$ are the weight factors of single scattering (SSC) and multiple scattering (MSC), respectively; T_α is the transmission at the sample orientation angle, α (here $\alpha = 45°$; $T_{45} = 0.85$). F_{bulk}, F^{in}_{hyd}, F^{out}_{hyd} (where "in" and "out" refer to water molecules in the CD cavity and outside), and F_{CD} are the intensity of $S_{bulk}(\vec{Q},\omega)$, $S^{in}_{hyd}(\vec{Q},\omega)$, $S^{out}_{hyd}(\vec{Q},\omega)$, and $S_{CD}(\vec{Q},\omega)$, respectively, and $F_{bulk} + F^{in}_{hyd} + F^{out}_{hyd} + F_{CD} = 1$. The concentration of CD solutions of 37.6 mM means that in average, 1 CD molecule is surrounded by a total number of 1477.7 water molecules, including bulk and hydration water; this is a representative unit of the CD solution (see Figure 2.1). In this unit, $F_{bulk} = n_{bulk}/n_{tot}$, $F^{in}_{hyd} = n^{in}_{hyd}/n_{tot}$, $F^{out}_{hyd} = n^{out}_{hyd}/n_{tot}$, $F_{CD} = n_{CD}/n_{tot}$, and $n_{tot} = n_{bulk} + n^{in}_{hyd} + n^{out}_{hyd} + n_{CD}$; where n_{bulk} , n^{in}_{hyd}, n^{out}_{hyd}, and n_{CD} are the numbers of H-atoms of the total, bulk, hydration water inside, outside the CD cavity, and CD, respectively. For individual CD solutions, while n_{tot}, n_{CD}, sum of n_{bulk} and n_{hyd} are temperature independent, n_{bulk}, n_{hyd} ($= n^{in}_{hyd}$ + n^{out}_{hyd}) vary with the temperature. The values of n_{tot}, n_{CD} are 3053.4 ($= 1477.7\times2 +$ 98), 98 for DIMEB; 3083.4, 128 for TRIMEG; 3035.4, 80 for γ-CD; see their chemical structure, Figure 1.11 (page 20).

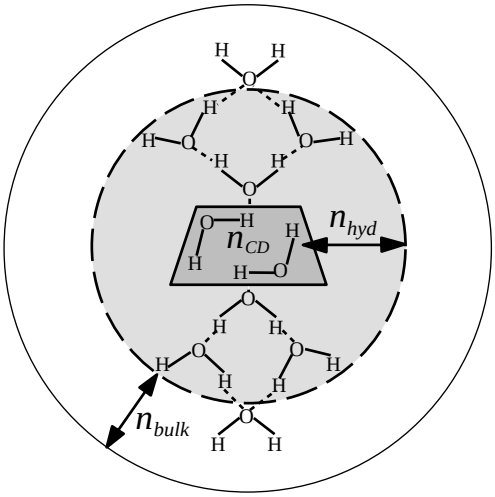

Figure 2.1: Schematic description of a CD solution representative unit
Analytical model for the line shape fitting can be separated into three fractions labeled with their corresponding numbers of H-atoms: fraction of CD (n_{CD}), fraction of hydration water (n_{hyd}), and fraction of bulk water (n_{bulk}). Note that n_{hyd} is subdivided to n_{hyd}^{in} and n_{hyd}^{out} which are the hydration water inside and outside the CD cavity, respectively.

The models of $S_{bulk}(\vec{Q},\omega)$, $S_{hyd}(\vec{Q},\omega)$, and $S_{CD}(\vec{Q},\omega)$ which have similar forms, are adopted and modified from Teixeira *et al.* [173] (by assuming that there is no coupling between the translational and rotational motions of the water molecules), i.e.,

$$S_{bulk}(\vec{Q},\omega) = S_{trans}(\vec{Q},\omega) \otimes S_{rot}(\vec{Q},\omega) \tag{2.8}$$

where $S_{trans}(\vec{Q},\omega)$ and $S_{rot}(\vec{Q},\omega)$ are the contributions from translational and rotational diffusion of bulk water, respectively. $S_{trans}(\vec{Q},\omega)$ is defined by

$$S_{trans}(\vec{Q},\omega) = \frac{1}{\pi}\frac{L_{trans}(\vec{Q})}{L_{trans}^2(\vec{Q})+\omega^2} \tag{2.9}$$

where $S_{trans}(\vec{Q},\omega)$ is a Lorentzian function with half width at half maximum (HWHM), $L_{trans}(\vec{Q}) = D_{trans}Q^2/(1+D_{trans}Q^2\tau_{trans})$, D_{trans} is the translational diffusion coefficient and τ_{trans} is the corresponding relaxation time. At low $\vec{Q}$-regime, $L_{trans}(\vec{Q}) = D_{trans}Q^2$ thus,

$$S_{trans}(\vec{Q},\omega) = \frac{1}{\pi}\frac{D_{trans}Q^2}{(D_{trans}Q^2)^2+\omega^2} \tag{2.10}$$

$S_{rot}(\vec{Q},\omega)$ is defined by

$$S_{rot}(\vec{Q},\omega) = A_0(\vec{Q})\delta\omega + \sum_{n=1}^{\infty} A_n(\vec{Q})L_n(\omega) \tag{2.11}$$

where $A_n(\vec{Q}) = (2n+1)j_n^2(\vec{Q}a)$, j_n^2 are the spherical Bessel functions with n = 1–3 ($n \geq 4$ are negligible), a denotes the radius of rotation which is 0.98 Å (for O–H distance of water molecule). $\delta(\omega)$ and $S_n(\omega)$ are the elastic-shaped and quasielastic Lorentzian components which have the corresponding intensities of the so called elastic incoherent structure factor ($A_0(\vec{Q})$ or EISF) and the quasielastic incoherent structure factors ($A_n(\vec{Q})$ or QISFs), respectively.

$$L_n(\omega) = \frac{1}{\pi}\frac{n(n+1)D_{rot}}{[n(n+1)D_{rot}]^2 + \omega^2} \tag{2.12}$$

have HWHMs of $n(n+1)D_{rot}$; D_{rot} is the rotational diffusion coefficient.

The convolution product of $S_{trans}(\vec{Q},\omega)$ (eqn 2.9) and $S_{rot}(\vec{Q},\omega)$ (eqn 2.11) is $S_{bulk}(\vec{Q},\omega)$ which can be written in a short form as:

$$S_{bulk}(\vec{Q},\omega) = \sum_{n=0}^{3} A_n(\vec{Q})L(X_n) \tag{2.13}$$

where $L(X_n)$ are the Lorentzians with HWHMs of X_n which are Q-dependent for translational diffusion ($n = 0$), and Q-independent for rotational diffusion (n = 1–3).

In analogy to eqn 2.13, $S_{hyd}^{in}(\vec{Q},\omega)$, $S_{hyd}^{out}(\vec{Q},\omega)$, and $S_{CD}(\vec{Q},\omega)$ (excluding MSC correction) can be stated as:

$$S_{hyd}^{in}(\vec{Q},\omega) = \sum_{k=0}^{3} A_k^{in}(\vec{Q})L(X_k^{in}) \tag{2.14}$$

$$S_{hyd}^{out}(\vec{Q},\omega) = \sum_{k=0}^{3} A_k^{out}(\vec{Q})L(X_k^{out}) \tag{2.15}$$

$$S_{CD}(\vec{Q},\omega) = \sum_{l=0}^{3} A_l^{CD}(\vec{Q})L(X_l^{CD}) \tag{2.16}$$

where the structure factors $A_k^{in}(\vec{Q})$, $A_k^{out}(\vec{Q})$, and $A_l^{CD}(\vec{Q})$ are given as:

$$A_k^{in}(\vec{Q}) = (2k+1)j_k^2(\vec{Q}a^{in}) \tag{2.17}$$

$$A_k^{out}(\vec{Q}) = (2k+1)[f_1^{out}j_k^2(\vec{Q}a_1^{out}) + f_2^{out}j_k^2(\vec{Q}a_2^{out})] \tag{2.18}$$

$$A_l^{CD}(\vec{Q}) = (2l+1)[f_1^{CD} j_l^2(\vec{Q}a_1^{CD}) + f_2^{CD} j_l^2(\vec{Q}a_2^{CD})] \tag{2.19}$$

a^{in} is the rotation radius of hydration water inside the CD cavity. For hydration water outside the CD cavity and CD itself with two different values of rotation radii a_1^{out}, a_2^{out} and a_1^{CD}, a_2^{CD} have their own respective weight factors f_1^{out}, f_2^{out}, and f_1^{CD}, f_2^{CD}. These values are obtained from the crystallographic data and are listed in Table 2.3. Note that the sum of weight factors of each component is equal to unity, i.e., $f_1^{out}+f_2^{out}=1$, $f_1^{CD}+f_2^{CD}=1$.

The scattering function of DHO, $S_{DHO}(\omega)$ is not a Lorentzian function:

$$S_{DHO}(\omega) = A_{DHO}(\vec{Q}) H_{DHO}(\omega) \tag{2.20}$$

where

$$A_{DHO}(\vec{Q}) = e^{\langle u^2\rangle_{DHO} Q^2} - 1 \tag{2.21}$$

$$H_{DHO}(\omega) = \frac{1}{\pi k_B T} \frac{\Gamma E^2}{(E^2-\omega^2)^2 + \omega^2\Gamma^2} \frac{\omega e^{-\frac{\omega}{k_B T}}}{1-e^{-\frac{2\omega}{k_B T}}} \tag{2.22}$$

E and Γ are the DHO energy and damping, respectively.

The most complex term is the MSC correction of bulk water:

$$\begin{aligned} S_{MSC}(\vec{Q},\omega) \;=\; & \frac{1-e^{-\langle u^2\rangle(4\pi/\lambda)^2}}{\langle u^2\rangle(4\pi/\lambda)^2} \{ \sum_{n=0}^{3}\sum_{m=0}^{3} A_n(\vec{Q}) AA_m(\vec{Q}_{90}) L(X_n+X_m) + \\ & H2_{DHO}(\omega)[A_n(\vec{Q})AA_{DHO} + AA_m(\vec{Q}_{90})A_{DHO}(\vec{Q}) + \\ & A_{DHO}(\vec{Q})AA_{DHO}]\} \end{aligned} \tag{2.23}$$

where $AA_m(\vec{Q}_{90}) = (2m+1)j_m^2(\vec{Q}_{90}a)$; this form is similar to that of $A_n(\vec{Q})$ in which $\vec{Q}$ is replaced by $\vec{Q}_{90}$ $(= 4\pi sin45^\circ/\lambda)$. The Lorentzian widths of the MSC terms are due to contributions only from translation and rotation:

$$\sum_{n=0}^{3}\sum_{m=0}^{3} L(X_n+X_m) = \sum_{n=0}^{3}\{[X_n + X_0(\vec{Q}_{90})] + [\sum_{m=1}^{3}(X_n+X_m)]\} \tag{2.24}$$

where $X_0(\vec{Q}_{90}) = D_{trans}Q_{90}^2/(1+D_{trans}Q_{90}^2\tau_{trans})$. For the contributions involving the DHO function, $H2_{DHO}(\omega)$ of the MSC part has DHO energy twice $H_{DHO}(\omega)$ of the SSC part (better approximation), i.e.,

$$H2_{DHO}(\omega) = \frac{1}{\pi k_B T} \frac{4\Gamma E^2}{(4E^2-\omega^2)^2 + \omega^2\Gamma^2} \frac{\omega e^{-\frac{\omega}{k_B T}}}{1-e^{-\frac{2\omega}{k_B T}}} \tag{2.25}$$

and

$$AA_{DHO} = \frac{e^{\langle u^2\rangle_{DHO}(4\pi/\lambda)^2} - 1}{\langle u^2\rangle_{DHO}(4\pi/\lambda)^2} - 1 \tag{2.26}$$

The contributions from inelastic scattering of vibrational motions of all components are taken into account by the global and DHO Debye-Waller factors (DWFs), $e^{-\langle u^2\rangle Q^2}$ and $e^{-\langle u^2\rangle_{DHO} Q^2}$ where $\langle u^2\rangle$ and $\langle u^2\rangle_{DHO}$ are the mean square displacements of three components (bulk, hydration water, CD) and DHO, respectively.

Because the main component of CD solution is the bulk water (> 90% of the total scattering intensity according to its number of H-atoms), it is necessary to obtain a good description of water dynamics at different temperatures (best fit with reasonable parameters) so that the dynamical parameters of the minor parts which are hydration water and CD can be determined precisely. The data analysis of CD solution starts from fitting between the measured scattering intensities and the theoretical models to determine dynamical parameters of pure water (for detail see below). Then the parameters of pure water are used as parameters of the bulk water component in the CD solution (see eqn 2.6) and fixed; therefore, only parameters of hydration water and CD are determined from the best agreement between $S_{theo}(\vec{Q},\omega)$ and $S_{meas}(\vec{Q},\omega)$ (for detail see below).

2.3.4.1 Fitting Steps of Pure Water Data

(i) The translational diffusion coefficients (D_{trans}) at different temperatures are fixed according to the precise values obtained by the pulsed field gradient (PFG)-NMR experiment (Dippel [37]):

$$D_{trans} = 90.32e^{-(573.287/T)^2}\ [10^{-5}\mathrm{cm^2 s^{-1}}] \tag{2.27}$$

(ii) The global and DHO mean square displacements are equal and are temperature dependent, i.e., $\langle u^2\rangle_{T_2} = \frac{T_2}{T_1}\langle u^2\rangle_{T_1}$. While $\langle u^2\rangle_{287}$ is determined by fitting, $\langle u^2\rangle_{305}$ and $\langle u^2\rangle_{323}$ are calculated by using the above relation and kept constant.

(iii) The other parameters, translational relaxation time (τ_{trans}), rotational diffusion coefficient (D_{rot}), DHO energy (E_{DHO}), and DHO damping (Γ_{DHO}) are obtained by fitting.

(iv) Because the data at 323 K is not good (the intensities of corrected spectra have dramatically decreased which is probably due to leaking of liquid from

the can during the measurement). Consequently, it cannot be used and its dynamical parameters are obtained by extrapolation using the values of the two lower temperatures (287 and 305 K), i.e., τ_{trans} and D_{rot} are determined by the Arrhenius Law:

$$(1/\tau_{trans})_T = (1/\tau_{trans})_\infty e^{-\frac{(E_a)_{1/\tau_{trans}}}{T}} \tag{2.28}$$

$$(D_{rot})_T = (D_{rot})_\infty e^{-\frac{(E_a)_{D_{rot}}}{T}} \tag{2.29}$$

(where $(E_a)_{1/\tau_{trans}}$ and $(E_a)_{D_{rot}}$ are the respective activation energies of $1/\tau_{trans}$ and D_{rot}) and E_{DHO}, Γ_{DHO} are obtained by a linear function.

2.3.4.2 Fitting Steps of CD Solution Data

(i) The dynamical parameters of bulk water are directly taken from the fitting results of pure water and are fixed, except for $\langle u^2 \rangle$ and DHO parameters which are allowed to be reoptimized if the fitting quality can be improved. However, $\langle u^2 \rangle$ and $\langle u^2 \rangle_{DHO}$ are set equal and are temperature dependent as in fitting of pure water, i.e., $\langle u^2 \rangle_{T_2} = \frac{T_2}{T_1} \langle u^2 \rangle_{T_1}$.

(ii) Assuming that the hydration water both inside and outside the CD cavity are hydrogen bonded to the CD macrocycle, forming a cluster and moving together in the solution, the hydration water and CD must have the same translational diffusion parameters.

$$D^{CD}_{trans} = D^{hyd}_{trans} \tag{2.30}$$

$$\tau^{CD}_{trans} = \tau^{hyd}_{trans} \tag{2.31}$$

(iii) For rotational diffusion, the hydration water molecules (both inside and outside the CD cavity) are assumed to be attached the CD macrocycle and they rotate together. Their rotation radii are obtained from the crystallographic data (DIMEB·15H_2O [9], TRIMEG·4.5H_2O [7], and γ-CD·14.1H_2O [63, 66]) using the histograms of the distribution of both hydration water and CD H-atoms from the center of mass (c.m.) of the CD macrocycle. It is found that while the hydration water inside the CD cavity have one rotation radius (a^{in}), the hydration water outside the cavity and CD itself have two different values (a^{out}_1, a^{out}_2; a^{CD}_1, a^{CD}_2); this reflects the predominant distribution of hydration

water and CD H-atoms at the primary and secondary sites of CD macrocycle with different weight factors, f_1^{out}, f_2^{out}; f_1^{CD}, f_2^{CD}. These values are given in Table 2.3, below.

$$D_{rot}^{CD} = D_{rot}^{hyd} \tag{2.32}$$

Table 2.3: Parameters for fitting obtaind from the crystallographic data
The rotation radii of hydration water (a^{in}, a_1^{out}, a_2^{out}) and CD (a_1^{CD}, a_2^{CD}) are given Å units. The corresponding weight factors, f_1^{out}, f_2^{out} for hydration water outside the CD cavity and f_1^{CD}, f_2^{CD} for CD, indicate the distribution of their H-atoms from the center of mass of CD macrocycle.

Sample	a^{in}	a_1^{out}	a_2^{out}	a_1^{CD}	a_2^{CD}	f_1^{out}/f_2^{out}	f_1^{CD}/f_2^{CD}
DIMEB	2.6	8.4	10.4	5.2	7.8	5/7	34/64
TRIMEG	2.7	9.1	11.3	6.0	8.8	1/2	46/82
γ-CD	2.9	8.9	10.4	5.8	7.9	4.5/6	34/46

The list of obtained parameters is given in Tables 3.5 (pure water), 3.6 (CD solutions) and the fitted spectra are shown in Figures B.1, B.2, B.3, and B.4 for pure water, DIMEB, TRIMEG, and γ-CD solutions, respectively.